

*promoting access to White Rose research papers*



**Universities of Leeds, Sheffield and York**  
**<http://eprints.whiterose.ac.uk/>**

---

This is an author produced version of a paper published in **Composites Science and Technology**

White Rose Research Online URL for this paper:  
<http://eprints.whiterose.ac.uk/2661/>

---

**Published paper**

Lee, J. and Soutis, C. (2007) *A study on the compressive strength of thick carbon fibre-epoxy laminates*, *Composites Science and Technology*, Volume 67 (10), 2015 -2026.

---

Elsevier Editorial System(tm) for Composites Science and Technology

Manuscript Draft

Manuscript Number: CSTE-D-06-00725R1

Title: A STUDY ON THE COMPRESSIVE STRENGTH OF THICK CARBON FIBRE-EPOXY LAMINATES

Article Type: Full Length Article

Section/Category:

Keywords: composites; compressive strength; size effects; manufacturing defects

Corresponding Author: Professor Constantinos Soutis, PhD

Corresponding Author's Institution: The University of Sheffield

First Author: Constantinos Soutis, PhD

Order of Authors: Constantinos Soutis, PhD; Jounghwan Lee, PhD

Manuscript Region of Origin:

Abstract: Abstract

This paper describes an experimental study that examines the effect of specimen size on the axial compressive strength of IM7/8552 carbon fibre/epoxy unidirectional laminates (UD). Laminate gauge length, width and thickness were increased by a scaling factor of 2 and 4 from the baseline specimen size of 10 mm x 10 mm x 2 mm. In all cases, strength decreased as specimen size increased, with a maximum reduction of 45%; no significant changes were observed for the axial modulus. Optical micrographs show that the failure mechanism is fibre microbuckling accompanied by matrix cracking and splitting. The location of failure in most specimens, especially the thicker ones, is where the tabs terminate and the gauge section begins suggesting that the high local stresses developed due to geometric discontinuity contribute to premature

failure and hence reduced compressive strength. Two generic quasi-isotropic multi-directional (MD) lay-ups were also tested in compression, one with blocked plies  $[45_n/90_n/-45_n/0_n]_s$  and the other with distributed plies  $[45/90/-45/0]_n$ s with  $n=2, 4$  and  $8$ . The material used and test fixture was identical to that of the unidirectional specimens with three different gauge sections ( $30\text{ mm} \times 30\text{ mm}$ ,  $60\text{ mm} \times 60\text{ mm}$  and  $120\text{ mm} \times 120\text{ mm}$ ) to establish any size effects. Strength results showed no evidence of a size effect when the specimens are scaled up using distributed plies and compared to the  $2\text{ mm}$  thick specimens. All blocked specimens had similar compressive strengths to the sub-laminate ones apart of the  $8\text{ mm}$  specimens that showed a  $30\%$  reduction due to extensive matrix cracking introduced during the specimen's cutting process. The calculated unidirectional failure stress (of the  $0^\circ$  ply within the multidirectional laminate) of about  $1710\text{ MPa}$  is slightly higher than the average measured value of  $1570\text{ MPa}$  of the  $2\text{ mm}$  thick baseline unidirectional specimen, suggesting that the reduced unidirectional strength observed for the thicker specimens is a testing artefact. It appears that the unidirectional compressive strength in thicker specimens ( $>2\text{ mm}$ ) is found to be limited by the stress concentration developed at the end tabs and manufacturing induced defects.

# A STUDY ON THE COMPRESSIVE STRENGTH OF THICK CARBON FIBRE-EPOXY LAMINATES

J. Lee and C. Soutis\*

Aerospace Engineering, The University of Sheffield

Mappin Street, Sheffield S1 3JD, UK

## Abstract

This paper describes an experimental study that examines the effect of specimen size on the axial compressive strength of IM7/8552 carbon fibre/epoxy unidirectional laminates (UD). Laminate gauge length, width and thickness were increased by a scaling factor of 2 and 4 from the baseline specimen size of 10 mm x 10 mm x 2 mm. In all cases, strength decreased as specimen size increased, with a maximum reduction of 45%; no significant changes were observed for the axial modulus. Optical micrographs show that the failure mechanism is fibre microbuckling accompanied by matrix cracking and splitting. The location of failure in most specimens, and especially the thicker ones, is where the tabs terminate and the gauge section begins suggesting that the high local stresses developed due to geometric discontinuity contribute to premature failure and, hence, reduced compressive strength. Two generic quasi-isotropic multi-directional (MD) lay-ups were also tested in compression, one with blocked plies  $[45_n/90_n/-45_n/0_n]_s$  and the other with distributed plies  $[45/90/-45/0]_{ns}$  with  $n=2, 4$  and  $8$ . The material used and test fixture was identical to that of the unidirectional specimens with

---

\* Corresponding author. Tel.: +44 (0)114 222 7811, Fax: 0044(0)114 2227836, c.soutis@sheffield.ac.uk

three different gauge sections (30 mm x 30 mm, 60 mm x 60 mm and 120 mm x 120 mm) to establish any size effects. Strength results showed no evidence of a size effect when the specimens are scaled up using distributed plies and compared to the 2 mm thick specimens. All blocked specimens had similar compressive strengths to the sub-laminate ones apart of the 8 mm specimens that showed a 30% reduction due to extensive matrix cracking introduced during the specimen's cutting process. The calculated unidirectional failure stress (of the 0° ply within the multidirectional laminate) of about 1710 MPa is slightly higher than the average measured value of 1570 MPa of the 2 mm thick baseline unidirectional specimen, suggesting that the reduced unidirectional strength observed for the thicker specimens is a testing artefact. It appears that the unidirectional compressive strength in thicker specimens (>2 mm) is found to be limited by the stress concentration developed at the end tabs and manufacturing induced defects such as fibre misalignment, ply waviness and voids.

**Keywords:** Composite laminates, Thick composites, Compressive strength, Manufacturing defects, Stress concentration, Size effects

## 1. Introduction

Considerable effort has been made over the years to understand the compressive behaviour and the mechanisms of compressive failure of thin (2mm - 3mm) unidirectional composite laminates. Numerous test methods and analytical models to predict the compressive strength have been developed. The models could be classified under two categories, i.e. microbuckling theories (Rosen<sup>1</sup>, Xu-Reifsnider<sup>2</sup> and Berbinau *et al*<sup>3</sup>) and fibre kinking theories (Argon<sup>4</sup>, Budiansky<sup>5</sup>, Lagoudas<sup>6</sup>). The test methods for thin specimens (2mm – 3mm) have been

classified according to the way the load is applied, i.e. direct end-loading (ASTM 695, CRAG and Wyoming End-loaded method), shear loading (Celanese, IITRI) and mixed shear/direct end-loading (Aerospatiale Test fixture and Imperial College ICSTM method)<sup>7</sup>.

Much less attention, however, has been paid to understand the compressive behaviour of thick unidirectional composite laminates even though requirement for advanced composite materials in thick structural sections (Airbus A380, Boeing 787) has significantly increased. This is caused by notorious difficulty of obtaining reliable test results. In fact, all problems related with compression testing become more serious and complicated with thicker composites, because of the tendency for premature failure due to global buckling or end crushing. In order to prevent the premature failure of the specimen, compression test specimens as well as test fixtures should be manufactured to provide a uniform one-dimensional compressive stress field, carefully considering the following factors: properties of the tabbing materials, tab bond characteristics, tab thickness and reliable specimen production procedures. Nevertheless, many workers often and mistakenly dismiss these factors as being of no importance. Of course, in addition to these parameters, specimen geometry, test fixture design and specimen misalignment in the fixture, can contribute to premature failures and reduced compressive strength values. Recent studies, Componeschi<sup>8</sup>, Hsiao<sup>9</sup>, Daniel<sup>10</sup> and Lee<sup>11</sup> made an effort to develop a suitable compression test method for thick composites and investigated the effect of specimen thickness on the compressive strength. It was found that the failure strength decreases with increasing thickness of the unidirectional laminate, but most of the failures occurred near or at the specimen end where the load is introduced (end crushing). It appears that existing test methods have not provided accurate and reproducible

compressive properties for the analysis and design of thick sections/structures. The need remains to develop a reliable compression test method for such thick constructions.

In terms of scaling of unidirectional laminates, the tendency of the thickness effects was revealed in the literature even though the thick specimens failed prematurely<sup>8-12</sup>. However, limited studies have been performed on 3-D scaling effects on the compressive strength, where all three dimensions are scaled up accordingly. In trying to explain the unexpected low failure strength of thick composites, possible explanations could fall into the categories of material or manufacturing related issues<sup>8</sup> and several questions can be raised. In terms of material aspects, the elastic constants or strength determined for thin laminates may not be applicable to thick composites. What are the trends for the compressive properties of composite materials with increasing thickness? In terms of manufacturing, does thickness change have an influence on fibre volume fraction, void content, ply or fibre waviness? If manufacturing quality were affected directly by the thickness change of the composite, a thickness effect would be expected since the compressive strength is governed by and is sensitive to these defects.

In the present study, a carefully thought procedure for the design of a thick compressive test specimens is presented. The cause of the premature failure of 2-8mm thick specimens made from the IM7/8552 carbon fibre/epoxy system is identified from experimental observations and numerical stress analysis. Stress concentration effects at the junction of the end tab and gauge section using plain and waisted specimens are investigated. The 3-D scaling effects on the compressive strength of IM7/8552 unidirectional laminates are systematically examined. In addition, two generic quasi-isotropic lay-ups are also tested in compression, one with blocked plies  $[45_n/90_n/-45_n/0_n]_s$  and the other with distributed plies  $[45/90/-45/0]_{ns}$  with

$n=2, 4$  and  $8$ . The calculated failure stress of the  $0^\circ$  ply in the multidirectional laminates is compared to that measured value for the  $0^\circ$  unidirectional laminate.

## **2. Experimental Procedure**

### **2.1 Material and lay-up**

The specimens were fabricated from commercially available (Hexcel Composites Ltd.) carbon/epoxy pre-impregnated tapes  $0.125\text{mm}$  thick. The tapes were made of continuous intermediate modulus IM7 carbon fibres pre-impregnated with Hexcel 8552 epoxy resin (34 vol % resin content). The material was laid up by hand in  $0.25\text{ m} \times 0.3\text{ m}$  unidirectional plates  $[0_4]_{ns}$  with  $n = 2, 3, 4$ , and  $8$  (i.e.,  $2, 3, 4$  and  $8\text{mm}$  thick). In addition, two quasi-isotropic lay-ups were fabricated, one with blocked plies  $[45_n/90_n/-45_n/0_n]_s$  and the other with distributed plies  $[45/90/-45/0]_{ns}$  with  $n=2, 4$  and  $8$  in order to gain an insight into the efficiency of  $0^\circ$  plies when employed in multidirectional laminates under uniaxial compression. The standard cure cycle recommended by Hexcel Composites Ltd was used for the thin laminates ( $< 4\text{mm}$  thick). The thicker laminates had to dwell in the autoclave for a longer period of time to allow even heat distribution throughout the panel and diminish the possibility of an exothermic reaction (heat energy that causes uncontrollable temperature rise within thick laminates). The in-plane stiffness and strength properties of the IM7/8552 unidirectional laminates provided by the materials manufacturer are presented in Table 1; values for the T800/924C carbon/epoxy system are provided for comparison purposes.

### **2.2 Specimen Geometry**

In order to develop a satisfactory procedure for the design of a compressive test specimen certain constraints need to be considered: i) end-tabs are required both to effectively transfer

load from the test machine grips to the specimen and to provide an adequate restraint against specimen buckling and brooming; ii) the overall specimen stability needs to be sufficient to ensure that compressive failure occurs significantly before potential buckling, implying correct combination of specimen length and flexural stiffness<sup>13</sup>.

The maximum allowable specimen gauge section length was determined on the basis of an Euler column buckling analysis assuming a pinned end strut with a rectangular cross-section and corrected to account for the influence of shear deflection due to transverse shear forces developed in anisotropic materials. Hence, for compressive failure to occur before Euler instability, the following condition must be satisfied<sup>14</sup>:

$$\sigma_{(ult)} \leq \frac{0.67k\pi^2(EI)}{AL^2} \quad (1)$$

where, E = longitudinal Young's modulus, I = second moment of area, A = cross-section area (Wt) and k is a constant taking into account the end support condition of the strut, i.e. the manner in which it is held. For a rectangular cross-section,  $I=At^2/12$ , and equation (1) can be expressed in terms of critical length (max allowable), L, as:

$$L_{max} \leq \pi \sqrt{\frac{0.67kE}{12\sigma_{(ult)}}} \quad (2)$$

For the current unidirectional composite system, assuming  $k = 1$  (a simply supported column, a conservative value) with E and  $\sigma_{(ult)}$  shown in Table 1, equation (2) gives an estimate of the critical length to avoid Euler buckling. Table 2 presents the critical length as a function of specimen thickness.

In order to avoid failure occurring at the junction of end-tab and the gauge section or within the tabs, then a specimen with waisted gauge section could be considered. Waisting the specimen through its thickness, which is in fact an optimised form of tabbing, has to be carried

out carefully in order to maintain a symmetric specimen, otherwise one would be likely to introduce bending and cause premature failure. Port<sup>15</sup> showed that interfacial splitting due to excessive shear stresses could be avoided when the specimen is waisted following the taper contour equation, which gives the minimum gauge length:

$$L_{\min} = \ln(t / t_0) \frac{\sigma_c}{\tau_c} t_0 \quad (3)$$

where  $L_{\min}$  is the minimum gauge length,  $t$  the nominal specimen thickness,  $t_0$  the minimum specimen thickness,  $\sigma_c$  is the compressive strength and  $\tau_c$  the shear strength. In practice it has been found necessary to allow for stress concentrations of up to 1.5 in order to produce failure in the test section and the required ratio of nominal thickness to waisted thickness is therefore 3:2.

For the IM7/8552 system assuming a compressive strength of 1690 MPa and shear strength of 110 MPa (Table 1) the minimum gauge length as a function of thickness is given in Table 3. The results presented in Table 2 show that for instance an 8mm IM7/8552 specimen with waisted gauge section to avoid Euler bending the gauge length has to be less than 55.9mm, but greater than 33.1mm (Table 3) since this will produce interlaminar and not compressive failure due to inadequate transfer length. To satisfy the conditions of both equations (2) and (3) the gauge length  $L_g$  of the specimen must lie between the limits:

$$L_{\min} \leq L_g \leq L_{\max} \quad (4)$$

Table 4 summarises the optimum gauge length for the plain and waisted specimen design as a function of laminate thickness, while Table 5 presents the final dimensions (gauge length x width x thickness) used for the IM7/8552 unidirectional specimens. The baseline specimen dimensions of 10mm x 10mm x 2mm (gauge length x width x thickness) were increased by a

scaling factor of 2 and 4. The selected dimensions satisfy the requirement to eliminate Euler buckling, avoid end tab effects and free edge effects. Table 6 shows the specimen geometry used for the multidirectional laminates. Three different gauge sections (30 mm x 30 mm, 60 mm x 60 mm and 120 mm x 120 mm) were tested to establish any size effects. All the specimens were bonded with 50 mm long woven glass fibre-epoxy reinforced end-tabs. After tabbing, individual specimens were machined to final tolerance by grinding the specimen ends and tab surfaces parallel within 0.025 mm (0.001 in).

### **2.3 Test fixture and mechanical Tests**

Generating a uniform one-dimensional stress state is the main objective of a compression test fixture. Stress concentrations due to load introduction present the most serious problems for unidirectional lay-ups and may cause premature failure of the specimen. Currently, there are no universally accepted test standards for testing specimens thicker than 2 mm. In the present study, compression tests on the unidirectional specimens were performed using the Imperial College ICSTM test jig<sup>7</sup> at a constant compression rate of 1 mm / min on a servo-hydraulic machine with a load capacity of 1000 kN, Figure 1. The ICSTM method uses a specimen configuration similar to the ASTM D695 specimen that is a tabbed specimen, which is loaded purely on the ends. However, a small amount (in the region of 10%) is applied by shear loading via the end-tabs, thus lowering the average stresses at the end of the test piece. The fixture consists of two grip blocks, Figure 1b that accommodate the specimen and prevent debonding of the tabs from the specimen end, shear failure of the end or compression failure under the tab, which are problems encountered with other test methods. The clamping blocks rest on hardened and ground steel plates, a measure that is necessary to avoid indentations of

the loading surfaces. The high precision die set shown in Figure 1a is commercially available and is designed to eliminate specimen misalignments. The lower grip is not attached to the lower plate of the die set in order to minimise additional constraints during testing, like bending of the specimen due to misalignment between the upper and lower grips. The bolt torque applied in the clamping blocks for the 2 mm thick specimen was in the region of 8-10 Nm and increased slightly for the thicker specimens. An advantage of the fixture is that by adjusting the size of the clamping blocks a variety of specimen sizes can be accommodated; it was also used to test multidirectional laminates.

Foil strain gauges were used on both faces of all specimens to be tested in order to monitor the degree of Euler bending and measure axial strain and, hence, axial modulus. The location and nature of damage in the UD laminates was obtained by optical and scanning electron microscopy (SEM) At least five specimens for each configuration were tested. Tables 5 and 6 show the systematic test matrix for the study of size effects on the strength of unidirectional and multidirectional laminates. An anti-buckling device was employed to restrain Euler bending<sup>11, 13</sup> in the testing of the multidirectional laminates.

### **3. Compressive Test Results**

The experimental results consist of stress-strain plots, fracture stresses and strains for the unidirectional and multidirectional laminates, scanning electron micrographs of some of the fracture surfaces, and photographs showing the overall failure mode of selected specimens. The end-tab thickness effects in unidirectional specimens were examined by performing a three-dimensional (3-D) finite element (FE) stress analysis using the commercially available package ANSYS. In the simulation of the end-loaded specimen, a 3-D eight-node solid

element (SOLID64) was employed to represent the tabs and the composite laminate; the bolt torque of 8-10 Nm applied in the clamping blocks of the ICSTM test fixture was represented by an equivalent lateral pressure in the FE analysis. One-quarter of the 20 mm x 20 mm x 4 mm unidirectional specimen were modelled with increasing end-tab thickness from 0.5 mm to 6 mm.

The compressive strength properties of the T800/924C carbon fibre-epoxy unidirectional specimens<sup>11</sup> are shown for comparison purposes.

### **3.1 Unidirectional laminates**

Initial compression tests on unidirectional specimens with relatively thin end tabs showed that failure occurred within the tabbed region, Figure 2, resulting in relatively lower compressive strengths (20-30% lower than expected). It appears that damage initiated on the end of the specimen (top corner) at the load introduction point and propagated down the length and across the width of the specimen. Due to the clamping constraining effect failure was progressive in nature, resulting in a more ‘ductile’ load-displacement curve, Figure 3, rather than the relatively brittle catastrophic failure that is usually observed when the specimen breaks within the gauge section or near the end tab. Optical microscopy images of the broken specimens reveal that the failure mechanism is that of fibre microbuckling or fibre kinking, Figure 4. Kink bands propagated through the thickness of the specimen (out-of-plane fibre microbuckling) and across the specimen width at an angle of 20 to 30° with a kink band width of approximately 90 µm (about 12 fibre diameters) similar to that reported in earlier studies<sup>11, 13</sup> for other carbon/epoxy systems.

As a result of these findings, ‘compression in tab’ type failure, the tab thickness was increased substantially see Table 5; the following results reported here are for such specimens. Representative stress-strain curves of 2mm (plot A), 4mm (plot B) and 8mm (plot C) thick unidirectional IM7/8552 specimens obtained at the centre of each specimen from back-to-back strain gauges are shown in Figure 5. Plots B for the 4 mm thick (32-ply) specimen and C for the 8 mm thick (64-ply) specimen are offset by 0.5% and 1.0% strain, respectively, so results can appear on the same graph.

The consistency of the two strain gauge readings up to failure in each curve indicates that bending due to misalignment has been successfully minimized. These three curves show similar stress-strain behaviour, which is essentially linear up to a strain level of approximately 0.5 %. Thereafter, the material behaves nonlinearly with a softening which increases with increasing applied load. The axial compressive modulus was determined at 0.25 % applied strain. The stress-strain curves illustrate that the axial modulus is independent of specimen size, Figure 5.

Compressive failure of the IM7/8552 unidirectional carbon-epoxy composite for all sizes was instantaneous and catastrophic and was accompanied by an audible acoustic event prior to the catastrophic failure. When failure occurred, the test piece broke into two pieces with fracture surfaces inclined at typical angles of between  $\beta = 5^\circ \sim 30^\circ$  ( $\beta$ : kinkband inclination angle) in the width direction (in-plane microbuckling) or thickness direction (out-of-plane microbuckling), see Figure 6a. After the compression tests, some of the broken specimens were selected and examined in the SEM. Figure 6b depicts the microscopic feature of a typical fracture surface, in which fibres break at two points, which creates a fibre kink band (in-plane microbuckling) inclined at angle  $\beta \sim 23^\circ$  to the horizontal axis. There is also little reason to

doubt that failure in general is by microbuckling of fibres because the characteristic kink band angle is similar to the fracture surface angle of test piece fragments (see Figure 6a), though usually slightly larger. Kink bands may start at the free edge or locations of stress concentration, such as, a pre-existing material defect or near the grips and propagate across the specimen width leading to catastrophic failure.

Of course, from the post failure examination of the broken specimens it can be seen that in addition to fibre microbuckling (a fibre instability failure mode) other damage mechanisms like matrix cracking and splitting are present, Figure 7. In most specimens, and especially the thicker ones, final fracture was located near the line where the end tab terminates and the gauge section begins suggesting that the high local stresses developed due to geometric discontinuity contribute to premature failure and, hence, reduced compressive strength, Table 6. It can be seen from Figure 8, which shows stress results from a three-dimensional ANSYS finite element stress analysis, that a 4 mm thick end tab would produce a stress concentration of approximately 1.7, explaining partly the premature failure of the thicker specimens. Using a thinner tab would cause a less severe discontinuity and reduced stress concentration factor (SCF) but wouldn't be stiff enough to transfer the compressive load effectively on thick specimens leading to compression failure under the tab as observed in Figure 2; in the 8 mm thick specimens loads in the region of 300 kN are applied before they fail. The failure stress and strain results for all IM7/8552 unidirectional specimens are summarised in Table 7 together with the equivalent values for the T800/924C system<sup>11</sup> for comparison purposes. The results show a sharp decrease in compressive strength with increasing thickness and volume. The strength of the T800/924C and IM7/8552 unidirectional laminate dropped by 36% and 45% in going from a 2 mm to 8 mm thick specimen, respectively. It should be noted that for the

T800/924C specimens only the thickness was varied while the gauge section (10 mm x 10 mm) remained unchanged. This may suggest that the width has a little effect, but in order to create a uniform one-dimensional stress field, avoiding grip and edge effects, the gauge length and specimen width should vary with increasing thickness and in the case of the IM7/8522 testing programme they were five times the specimen thickness. However, the 4 mm and 8 mm thick specimens still failed prematurely, but this is explained by the effect of tab induced stress concentrations in addition to reduced fibre volume fraction, increased ply waviness and fibre misalignment and increased void content that may occur with increasing specimen thickness, see below in section 4.

In the effort to quantify the tab effect and avoid near grip failures, three 8 mm thick unidirectional specimens with waisted gauge section were tested. They had a gauge section of 20 mm x 40 mm and a reduced thickness of 5.5 mm, Figure 9a. Overall fracture occurred almost in the middle of the gauge section in the form of fibre breakage and axial splitting. Although this can be considered as a successful test with a valid failure mode (away from the end tabs) the average compressive strength of 1118 MPa (22% higher than the value reported for the plain 8 mm thick test piece) is at least 30% lower than the strength measured for the standard 10 mm x 10 mm x 2 mm specimen (1570 MPa), suggesting that the thickness and other related factors are affecting its ultimate strength. It may not be possible to achieve the same compaction, removal of voids or cure uniformity for the thick laminates compared with the thinner ones. The need to avoid overheating due to the exothermic cure is well recognised and documented.

### 3.2. Multidirectional laminates

Two generic multidirectional quasi-isotropic lay-ups were studied, one with blocked plies  $[45_n/90_n/-45_n/0_n]_s$  (ply-level scaling) and the other with distributed plies  $[45/90/-45/0]_{ns}$  (sublaminates-level scaling) with  $n=2, 4$  and  $8$  in order to gain an insight into the efficiency of  $0^\circ$  plies when employed in multidirectional laminates under uniaxial compression. The specimen geometries tested are presented in Table 6; at least five specimens were tested per configuration. The lay-up was chosen with off-axis plies on the outside, as they are an important constituent element in most structural components where damage resistance and tolerance is a requirement.

Typical stress-strain curves of the 2mm, 4mm and 8mm thick multidirectional specimens laminated with sublaminates level and ply level stacking sequences are shown in Figure 10a and 10b, respectively. Plots B for the 4 mm thick specimen and C for the 8 mm thick specimen are offset by 0.5% and 1.0% strain, respectively.

The nonlinearity of the multidirectional specimens is higher than that of the  $0^\circ$  longitudinal ones (see Figure 5) due to non-linear behaviour of the off-axis layers. The average failure strain ( $\sim 1.3\%$ ) of the multidirectional specimens is generally higher than that of the  $0^\circ$  unidirectional ones, suggesting that the mechanism of failure in the axial plies is affected by the adjacent off-axis plies. The off-axis layers provide lateral support to the  $0^\circ$  axial plies that delay the initiation of fibre microbuckling. They also reduce the stress concentration factor in the end tab region (more compliant layers) avoiding premature grip failures. The measured elastic moduli at a 0.25 % applied strain are in reasonable agreement when compared with that estimated by the laminate plate theory (58 GPa for the multidirectional IM7/8552 laminate).

All specimens failed within the gauge section, Figure 11; Table 8 shows that the compressive strengths were similar for both lay-ups with an average value of 657 MPa, apart of the 8 mm thick ply-level scaled  $[45_8/90_8/-45_8/0_8]_s$  laminate that failed at 472 MPa due to edge delamination rather than  $0^\circ$  fibre breakage. Extensive matrix cracking that was introduced during the cutting process of the test pieces could contribute to the initiation of edge delamination and premature specimen failure. It is thought that the matrix cracks shown in Figure 12 were due to the trapped thermal stresses, something that needs to be further investigated.

The ultimate stress in the  $0^\circ$  plies in these quasi-isotropic multidirectional laminates at the ultimate compressive failure of the laminate ( $\sim 657$  MPa), has been obtained from a simple stiffness ratio method (or the maximum stress failure criterion) and found equal to 1710 MPa, which is approximately 10 % higher than the strength obtained from the 10 mm x 10 mm x 2 mm standard unidirectional specimen. A possible explanation is that the off-axis plies protect the load carrying  $0^\circ$  layers from the stress concentrations at the tabs so managing to come closer or achieve their intrinsic strength. Compressive strength results of  $[0/0/90]_{ns}$  laminates reported in reference [8] showed a decrease in strength of approximately 22% from 6.4 mm to 25.4 mm thick specimens. All failures occurred at the gauge length-tab termination interface due to high local stress as explained above for the IM7 system. Having the  $0^\circ$  plies on the surface fibre kinking is triggered earlier causing premature failures.

In the 8 mm thick IM7/8552 blocked laminate the  $0^\circ$  plies experienced a stress of only 1227 MPa when the laminate failed at 472 MPa, but this has been affected by the existing matrix crack damage as discussed earlier. It should also be noted, in Table 8, that the strength coefficient of variation for the laminate with the blocked plies was quite high (19% compared

to 3-7% for the laminate with the distributed layers) implying a higher content of manufacturing defects like voids and ply/fibre waviness. There was also a tendency of failures to occur near the grip for the  $n \geq 4$  specimens suggesting that blocking the plies makes the laminate more susceptible to stress concentrations developed in the tab region.

#### **4. Parameters influencing the compressive strength**

The influence of fibre volume fraction on the mechanical properties of composites under compressive load is reasonably well understood<sup>18,19</sup>. Thicker laminates tend to have a lower fibre volume fraction and for an 8 mm thick T800/924C unidirectional specimen manufactured by the authors<sup>11</sup> dropped by about 7% when compared to a 2 mm thick specimen. The void content also increases with increasing laminate volume and the presence of gaps and voids greatly affect the initiation of damage (triggering of fibre microbuckling) and result in reduced laminate strength. Figure 13 shows the average void content of T800/924C unidirectional  $[0_4]_{ns}$  laminates ( $n=2, 4$  and  $8$ ) as a function of specimen thickness. It can be seen from Figure 13 that the void content increases with increasing specimen thickness. The fibre and void content in these laminates were measured by using the resin acid digestion test suggested by BAE Systems<sup>20</sup>.

Fibre waviness is another manufacturing defect that can detrimentally reduce the compressive load carrying capability of unidirectional and multidirectional laminates. It can be introduced during the fabrication (filament winding, weaving, braiding) and curing processes of UD pre-pregs and can be further enhanced in thicker components during manufacturing. Yugaris<sup>17</sup> identified that the lamination process can change the fibre misalignment distribution and different resin flow fields found in different composite systems could lead to

changes in the distributions, hence differences in mechanical properties. The misalignment angle associated with fibre waviness has been reported to significantly influence longitudinal compressive strength<sup>5,10,11</sup>.

In earlier work by the authors, the extent of the fibre waviness was investigated according to the specimen thickness (2mm, 4mm and 8mm) and compared with the standard deviation,  $\sigma$ , of the fibre angle distribution. The major axis' length of 1000 fibres for each sample were measured to calculate the in-plane fibre misalignment angle. Figure 14 shows the fibre waviness distribution of T800/924C unidirectional specimens  $[0_4]_{ns}$  as a function of specimen thickness ( $n=2, 4$  and  $8$ ). The distribution for the 8mm thick specimen is clearly wider ( $\sigma = 1.90^\circ$ ) than those for the 2mm ( $\sigma = 0.90^\circ$ ) and 4mm thick specimen ( $\sigma = 0.92^\circ$ ). The wider distribution means poorer fibre alignment in the specimen. This may be caused by the movement of fibres during the curing process, i.e., fibres are more likely to move due to the factors such as the fibre nesting and resin flow or resin release in the thicker unidirectional laminate.

Unfortunately, there is no mathematical model that can quantitatively describe or predict the strength of the laminate as a function of fibre volume fraction, void content, fibre misalignment and thickness. However, from the measured data presented in Table 6 it is observed that the compressive strength of the unidirectional laminate can be described by the following empirical relationship:

$$\sigma_{ult} = \sigma_c^{st} t^{-\alpha} \quad (5)$$

where  $\sigma_c^{st}$  is the measured compressive strength of the baseline 2 mm thick specimen (=1570 MPa for the IM7/8552 system),  $t$  is the thickness of the specimen and the exponent  $\alpha$  is equal to 0.25. Thickness  $t$  in equation (5) implicitly accounts for the above-mentioned

manufacturing defects without of course giving the exact contribution of each parameter. It should be also noted that the measured strengths are affected by end tab stresses. Equation (5) is similar to that described by Niklewicz and Sims<sup>21</sup> who studied recently size effects in carbon fibre/vinylester and carbon/epoxy systems. The unidirectional specimens examined in their study<sup>21</sup> also failed by the stress concentrations induced by end tabs. Niklewicz and Sims<sup>21</sup> FE analysis showed that the standard un-tapered tab produced a stress concentration in the specimen of approximately 1.7, which is similar to the value estimated in the present investigation.

The fibre microbuckling model by Budiansky<sup>5</sup> can directly account for initial fibre waviness and indirectly for void content that affects the in-plane shear strength of the composite. The longitudinal compressive strength can be estimated as a function of fibre waviness and shear strength properties by the following expression

$$\sigma = \frac{\tau_y^*}{\phi_0 + \gamma_y} \quad (6)$$

where  $\phi_0$  is the initial fibre waviness angle in the kink band,  $\gamma_y$  is the yield shear strain and  $\tau_y^*$  is given by:

$$\tau_y^* = \tau_y \left[ 1 + \left( \frac{\sigma_{Ty}}{\tau_y} \right)^2 \tan^2 \beta \right]^{\frac{1}{2}} \quad (7)$$

with  $\tau_y, \sigma_{Ty}$  and  $\beta$  are the in-plane shear yield strength, transverse yield strength and kink band inclination angle of the composite, respectively. Using this model, one can estimate the variation of compressive strength as a function of fibre imperfections for the T800/924C and IM7/8552 materials systems, Figure 15. In this figure the experimentally - correlated compressive strengths are compared with the measured experimental values. The measured

compressive strengths of 1625 MPa for the 2mm thick T800/924C and 1570 MPa for the IM7/8552 laminate correspond to an initial fibre waviness of  $\phi_0 \cong 1.17^\circ$  and  $\phi_0 \cong 1.27^\circ$ , respectively. For the 8mm thick specimens, the measured compressive strengths of 1087 MPa for the T800/924C and 869 MPa for the IM7/8552 system are in accord with an initial fibre waviness of  $\phi_0 \cong 2.31^\circ$  and  $\phi_0 \cong 3.19^\circ$ , respectively. The average fibre misalignment measured<sup>11</sup> in accordance with Yurgartis method<sup>17</sup> varied from approximately  $1^\circ$  to  $2^\circ$  with increasing specimen thickness (2mm to 8mm thick), Figure 14. The message here is that the compressive strength of UD laminates is very sensitive to fibre misalignment and even values of  $2\text{-}3^\circ$  can cause a strength reduction of up to 40%. Need also to note that, although the microbuckling model or a Weibull statistics approach can be used to obtain similar strength values for the UD laminates, the final failure of the larger volume specimens tested here is dramatically affected by the stress concentrations induced by the end-tabs. Using  $45^\circ$  and  $90^\circ$  plies as outer layers can reduce these high tab stress concentrations helping the  $0^\circ$  plies to achieve their intrinsic compressive strength and valid compressive failures within the specimen gauge section as discussed earlier in section 3.2.

## 5. Discussion

It is acknowledged that measuring the mechanical properties of continuous carbon fibre reinforced laminates, unidirectional or multidirectional, under uniaxial compression is a cumbersome task and more so for thicker ( $>2$  mm) specimens. The lack of success is evident in the large number of test methods and specimen designs that have been proposed over the last 30 years. In addition to specimen design (Euler buckling, interlaminar shear failure) and test fixture the operator, specimen misalignment in the testing jig, quality of material and non-

uniform loading can influence compression testing. Generating a uniform one-dimensional stress state is the main objective of a compression test fixture and in the present study this was resolved by employing the Imperial College ICSTM test jig that uses a specimen configuration similar to the ASTM D695 test piece that is tabbed and is loaded purely on the ends. The specimens' dimensions for the thin and thicker specimens were carefully selected to avoid invalid failures due to Euler buckling, end or edge effects. The gauge length and width were five times the specimen thickness with appropriate tab thickness to avoid 'compression in tab' type failures. However, eliminating stress concentrations in specimens as a result of load introduction and manufacturing defects in the form of voids, fibre volume fraction, ply waviness and fibre misalignment with increased specimen size has proved to be more troublesome.

Figure 16 summarises the compressive strengths for the T800/924C and IM7/8552 UD systems showing a sharp decrease in strength with increasing specimen thickness and volume. In this figure, for the T800/924C the thickness of the baseline specimen (10mm x 10mm x 2mm) was increased to 3mm, 4mm and 8mm, while the dimensions of the IM7/8552 specimen were scaled by a factor of 2 and 4. A strength reduction of 36% and 46%, in going from 2mm to 8mm thick specimens, is observed for the two systems, respectively. This is mainly attributed to the SCF developed along the line where the end tab terminates and the gauge section begins. Multiplying the average failure stress of 869 MPa for the IM7/8552 UD specimen, Figure 16, by a SCF value of 1.8 that has been estimated by the finite element analysis in Figure 8, a compressive strength of 1564 MPa is obtained that corresponds to that measured for the 2 mm thick baseline specimen. Of course, using partly bonded end tabs<sup>7</sup>, thinner end tabs or specimens with a waisted gauge section can reduce the SCF, but other

problems arise complicating the picture. It should also be said that even the measured strength of the 2 mm thick specimen is not necessarily the actual ultimate value but represents a lower bound of the intrinsic strength, since grip or near grip failures still occur. Fibre microbuckling or fibre kinking was identified as the critical failure mechanism, but matrix cracking and splitting accompanied final failure.

The compression tests that were carried out on the two generic IM7/8552 quasi-isotropic multi-directional lay-ups, one with blocked  $[45_n/90_n/-45_n/0_n]_s$  and the other with distributed plies  $[45/90/-45/0]_{ns}$ , with  $n=2, 4$  and  $8$  showed no strength reduction with increasing specimen volume (size) apart of the 8 mm thick ply-level scaled specimens that failed prematurely due to pre-existing matrix cracking damage introduced during the specimen cutting process by the released thermal stresses, Table 8. All specimens failed within the gauge section suggesting that the ICSTM test fixture and specimen design were very much appropriate. The ultimate stress of the  $0^\circ$  plies in the multidirectional laminates at the ultimate compressive failure of the laminate was estimated from the laminate plate theory together with the maximum stress failure criterion and found equal to 1710 MPa, which is 10% higher than the measured value of the 2 mm thick baseline specimen. Alternatively, it could be simply obtained by multiplying the laminate strain at failure ( $\sim 1.3\%$ ) by the modulus of the  $0^\circ$  plies ( $\sim 150$  GPa) assuming that the strain in the  $0^\circ$  layers is the same as the laminate strain. This would result to an ultimate compressive stress for the  $0^\circ$  plies of 1950 MPa, which is 20% higher than the measured UD strength. It appears that by using  $45^\circ$  and  $90^\circ$  as outer plies reduce the tab stress concentration and provide appropriate lateral support to the  $0^\circ$  load carrying layers enabling them to achieve failure stresses closer to their intrinsic compressive strength. Ply-level scaled laminates performed as well as the laminates with the distributed

plies (sublaminates-level scaling) provided that no more than 4 plies of the same orientation were blocked together.

The strength reduction in unidirectional specimens with increasing specimen thickness and volumes could, therefore, be attributed to stress concentrations developed at the end tabs and manufacturing defects in the form of void content, ply waviness and fibre misalignment that could be enhanced in thicker laminates.

## **6. Concluding remarks**

The influence of the test operator and compression jig has a great effect on the measured strength properties. In the present study careful specimen design/preparation and the employment of the ICSTM test fixture<sup>7</sup> enabled us to perform successfully compression testing of relatively thick UD and MD carbon fibre/epoxy laminates. However, stress concentrations present the most serious problems for unidirectional lay-ups and do cause premature failures of the specimen resulting in low compressive strengths. The following guidelines could be followed to minimise the testing artefact:

- (i) The specimen gauge length and width should be at least 5 times the thickness to ensure that end tab and free edge effects are avoided and compressive failure occurs significantly before potential Euler buckling, implying a correct combination of specimen gauge section and flexural stiffness.
- (ii) End tabs should be of sufficient length (in this case at least 50 mm long) and thickness should be similar to the specimen thickness to eliminate ‘compression in tab’ type failures that lead to artificially low compressive strength values.

- (iii) Multidirectional quasi-isotropic laminates with preferably a distributed ply stacking sequence could be used to evaluate the unidirectional compressive strength and study size effects.
- (iv) Use of 45° and 90° plies as outer layers reduce dramatically the tab stress concentration helping to achieve valid compressive failures within the specimen gauge section.
- (v) Ply-level scaled quasi-isotropic laminates could also be used to study size effects but no more than 4 plies of the same orientation (and definitely less than 8) should be blocked together. The 8 mm thick laminate  $[45_8/90_8/-45_8/0_8]_s$  failed due to matrix cracking and edge delamination rather than fibre fracture.

## **7. Acknowledgments**

The authors gratefully acknowledge the support of the UK Engineering and Physical Sciences Research Council (Grant No. GR/R89479/01), the UK Ministry of Defence, Airbus UK and Smiths Aerospace as well as the supply of material by Hexcel Composites.

## 8. References

1. Rosen, B. W., "Mechanics of composite strengthening", *Fibre Composite Materials*, American Society for Metals, 1965, pp. 37-75.
2. Xu, Y.L., Reifsinder, K.L., "Micromechanical modelling of composite compressive strength", *Journal of Composite Materials*, 1993, **27**(6), pp. 572-88.
3. Berbinau, P., Soutis, C. and Guz, I. A., "Compressive failure of 0° unidirectional carbon-fibre-reinforced plastic (CFRP) laminates by fibre microbuckling", *Composites Science and Technology*, 1999, **59**(9), pp. 1451-1455.
4. Argon, A. S., "Fracture of composites", *Treatise of Material Science and Technology*, Vol. 1, Academic Press, New York, 1972.
5. Budiansky, B., "Micromechanics", *Computers and Structures*, 1983, **16**(1-4), pp.3-12.
6. Lagoudas, D. C. and Saleh, A. M., "Compressive failure due to kinking of fibrous composites", *Journal of Composites Materials*, 1993, **27**(1), pp. 83-106.
7. Matthews, F. L. and Haberle, J. G. "A new method for compression testing", *European Conference on Composites Testing And Standardisation*, Sept. 8-10 1992, Amsterdam, Netherlands, pp. 91-99
8. Camponeschi, E. T., "Compression testing of thick-section composite materials", *Composite Materials: Fatigue and Fracture (Third Volume)*, ASTM STP 1110, American Society for Testing and Materials, Philadelphia, 1991, pp. 439-456.
9. Hsiao, H. M., Daniel, I. M. and Wooh, S. C., "A new compression test methods for thick composites", *Journal of Composite Materials*, 1995, **29**(13), pp. 1789-1806.

10. Daniel, I. M. and Hsiao, H. M., "Is there a thickness effect on compressive strength of unnotched composite laminates?", *International Journal of Fracture*, 1999, **95** (Special Issue), pp. 143-158.
11. Lee, J. and Soutis, C., "Thickness effect on the compressive strength of T800/924C carbon fibre-epoxy laminates", *Composites Part A*, **36**(2), 2005, pp. 213-227
12. Bazant, P. Z., Kim, J. H., Daniel, I. M., Emilie, B. G. and Zi, G., "Size effect on compression strength of fibre composites failing by kink band propagation", *International Journal of Fracture*, 1999, **95** (Special Issue), pp. 103-141.
13. Soutis, C. "Measurement of the static compressive strength of carbon fibre/epoxy laminates". *Composites Science & Tech.*, 1991, **42**(4), pp. 373-392
14. Whitman, J.M. and Pagano, N.J. "Shear deformation in heterogeneous anisotropic plates". *J Appl. Mech.*, 1970, **37** (4).
15. Port, K. F., "The compressive strength of CFRP", RAE Technical Report 82083, 1982.
16. Faupel, J. H. and Fisher, A. E., "Engineering design: a synthesis of stress analysis and materials engineering", 2<sup>nd</sup> Edition, John Wiley & Son, 1980.
17. Yugartis, S. W., "Measurement of small angle fibre misalignments in continuous fibre composites", *Composite Science and Technology*, **30**(4), 1987, pp. 279-293.
18. Kim, C. and White, S. R., "The continuous curing process for thermoset polymer composites. Part 2: Experimental Results for a Graphite/Epoxy Laminate", *Journal of Composite Materials*, 1996, **30**(5), pp. 627-647.
19. Chim, E. S. and Lo, K. H., "Compressive strength of unidirectional composites", *Journal of Reinforced Plastics and Composites*, 1992, **11**(8), pp. 838-896.

20. British Aerospace, “Test methods for the fibre and void content of cured carbon and glass fibre composites”, BAER 3014, Issue 3, 1990.

21. Niklewicz, J. and Sims, G.D. “Size effects in composite materials”. Structural Integrity and Performance Project CPD1, National Physical Laboratory, NPL Report MATC (A) 74, January 2002.

Table 1 Elastic Properties of the IM7/8552 and T800/924C systems

Property	E <sub>11</sub> GPa	E <sub>22</sub> GPa	G <sub>12</sub> GPa	ν <sub>12</sub>	σ <sub>11C</sub> MPa	σ <sub>22C</sub> MPa	τ <sub>12#</sub> MPa
IM7/8552	150	11.0	4.6	0.30	1690	250	120
T800/924C	161	9.25	6.0	0.35	1615	250	105

(σ<sub>11C</sub> = longitudinal compressive strength and σ<sub>22C</sub> = transverse compressive strength, τ<sub>12#</sub>=in-plane shear strength)

Table 2 Critical gauge lengths for the IM7/8552 UD plain specimens

Thickness /mm	2	4	6	8	10
L <sub>max</sub> /mm	13.9	27.6	45.9	55.9	69.9

Table 3: Minimum gauge length for the IM7/8552 UD waisted specimens

t/mm	2	4	6	8	10
t <sub>0</sub> /mm	1.34	2.67	4	5.34	6.67
L <sub>min</sub> /mm	8.2	16.6	24.9	33.1	41.5

Table 4: Specimen geometry for IM7/8552 thick plain and waisted specimens

t/mm	t <sub>0</sub> /mm	L <sub>g</sub> /mm
2	1.34	8.2 ≤ L <sub>g</sub> ≤ 13.9
4	2.67	16.6 ≤ L <sub>g</sub> ≤ 27.6
6	4.0	24.9 ≤ L <sub>g</sub> ≤ 45.9
8	5.34	33.1 ≤ L <sub>g</sub> ≤ 55.9
10	6.67	41.5 ≤ L <sub>g</sub> ≤ 69.9

Table 5: Dimensions for the IM7/8552 UD plain specimens

Dimension/mm	16-ply	32-ply	64-ply
Total length	110	120	140
Gauge length	10	20	40
Width	10	20	40
Nominal thickness	2.04	4.06	8.3
End-tab thickness	1.2	2.3	5
Modified tab thickness	3.1	6.0	10.0

**Note:** Dimensions (gauge length x width x thickness) of the 8mm specimen with a waisted gauge section were: 20 mm x 40 mm x 5.5 mm.

Table 6 Compression test programme for the unnotched MD specimens (Unit: mm)

Material	Quasi-isotropic lay-up	Thickness	Gauge length x width	Tab length
Pre-preg IM7/8552	Sublamine level scaling/ Ply level scaling	2	30 × 30	50
		4	60 × 60	50
		8	120 × 120	50

(End-tab material: Woven glass fibre-epoxy system)

Table 7. Average compressive properties of T800/924C and IM7/8552 UD laminates

Material	1-D thickness effect				
T800/924C	Dimensions (mm)	10 × 10 × 2	10 × 10 × 3	10 × 10 × 4	10 × 10 × 8
	Young's modulus GPa	167	164	164	161
	Failure strain, %	0.97	0.98	0.95	0.92
	Failure stress, MPa	1625	1602	1419	1069
	C.V.	4.79	7.08	1.07	2.32
Material	3-D size effect				
IM7/8552	Dimensions (mm)	10 × 10 × 2	20 × 20 × 4	40 × 40 × 8	
	Young's modulus GPa	156	151	158	
	Failure strain, %	1.3	0.96	0.61	
	Failure stress, MPa	1570	1253	869	
	C.V. (%)	4.51	6.60	6.03	

Table 8 Unnotched average compressive strengths of IM7/8552 sublamine-level ( $[45/90/-45/0]_{ns}$ ) and ply-level scaled specimens ( $[45_n/90_n/-45_n/0_n]_s$ )

Stacking sequence	Specimen thickness (mm)	Gauge length x Width		
		30mm x 30mm	60mm x 60mm	120mm x 120mm
$[45/90/-45/0]_{ns}$	2	658 MPa (3.15)	-	-
	4	-	675 MPa (6.6)	-
	8	-	-	644 MPa (14.0)
$[45_n/90_n/-45_n/0_n]_s$	2	666 MPa (19.6)	-	-
	4	-	642 MPa (19.0)	-
	8	-	-	472 MPa (13.4)*

( ): Coefficient Variation, %

\* Overall failure due to matrix cracking and edge delamination



**Figure 1** a) ICSTM compression test fixture and b) clamping blocks for a 40 mm x 40 mm x 8 mm specimen

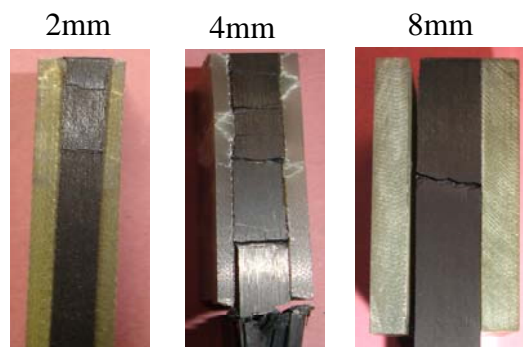


**Figure 2.** Post failure mode of IM7/8552 unidirectional specimens with relatively thin end tabs. 'Compression in tab' type failure.

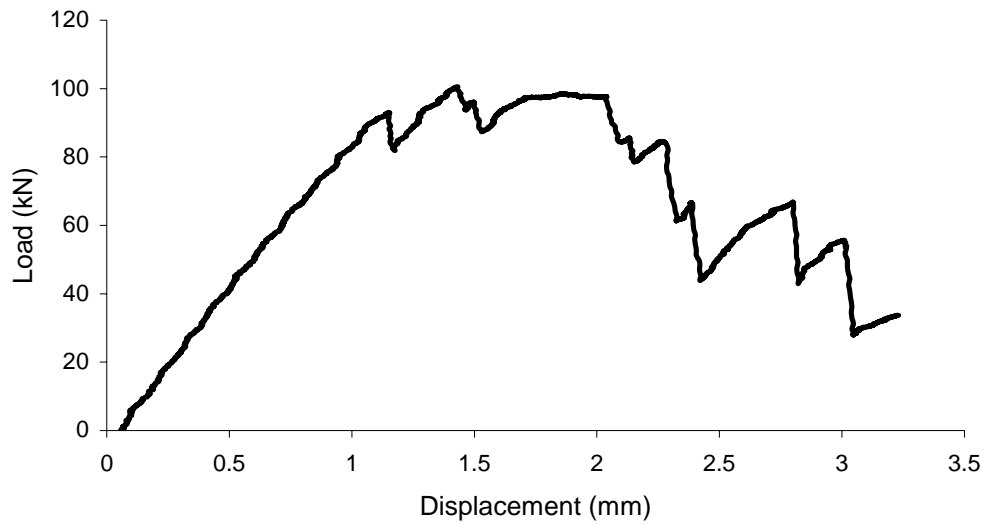


**Figure 3.** Typical load - displacement curve of a 4mm thick IM7/8552 UD specimen that failed within the tabbed region.

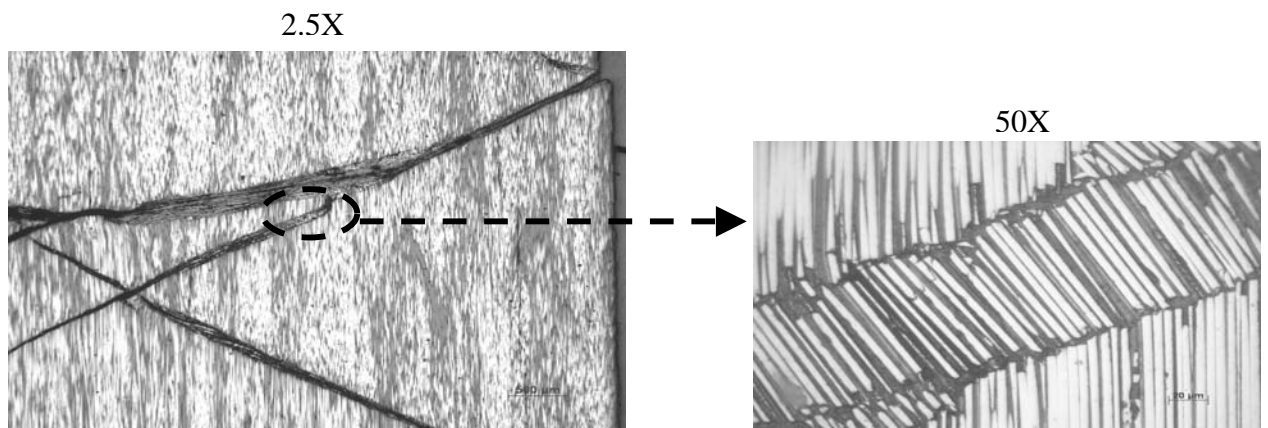


**Figure 4.** a) Optical micrograph of a 2mm thick IM7/8552 UD specimen that failed prematurely within the tab region. b) higher magnification of (a) showing clearly the fibre kink band or fibre microbuckling.

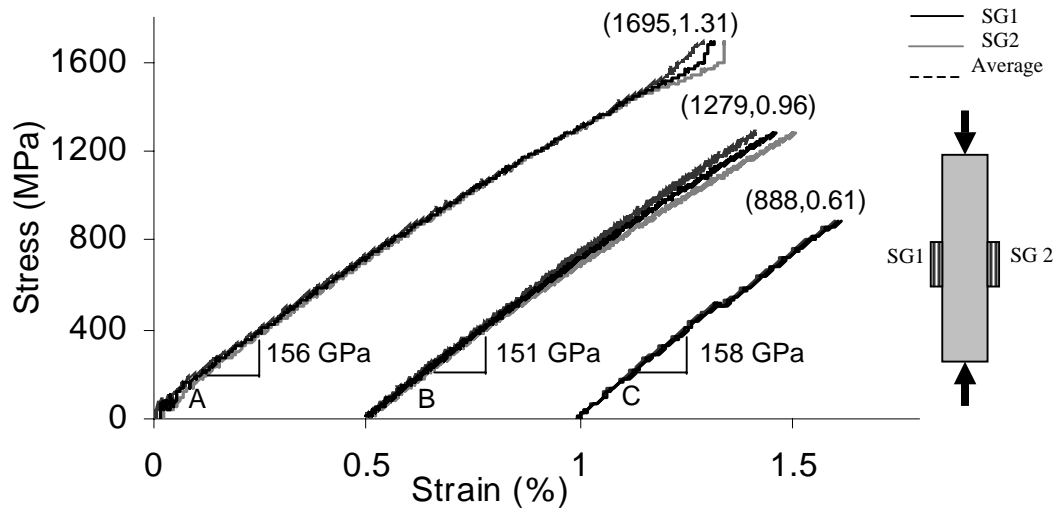


**Figure 5.** Typical stress-strain curves of the IM7/8552 unidirectional specimens obtained from back-to-back strain gauges (A: 10mm × 10mm × 2mm, B: 20mm × 20mm × 4mm and C: 40mm × 40mm × 8mm.)

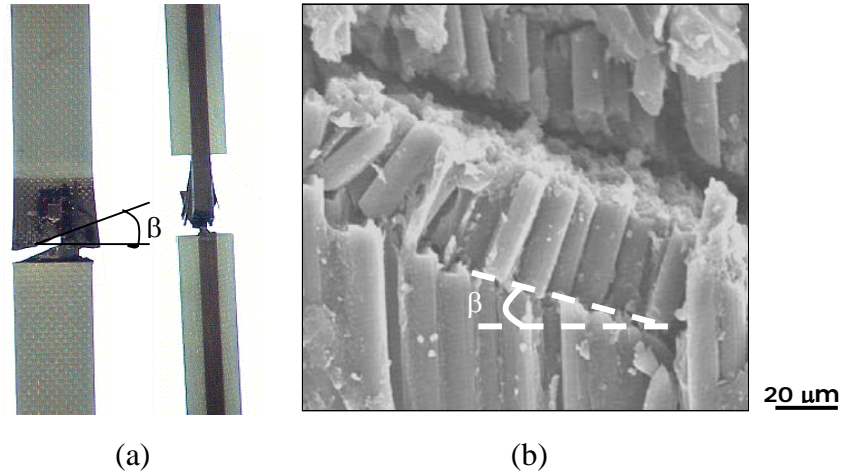


**Figure 6.** a) Typical overall failure mode of a UD specimen and b) an SEM micrograph of fibre kinking (specimen dimensions: 10mm × 10mm × 2mm).

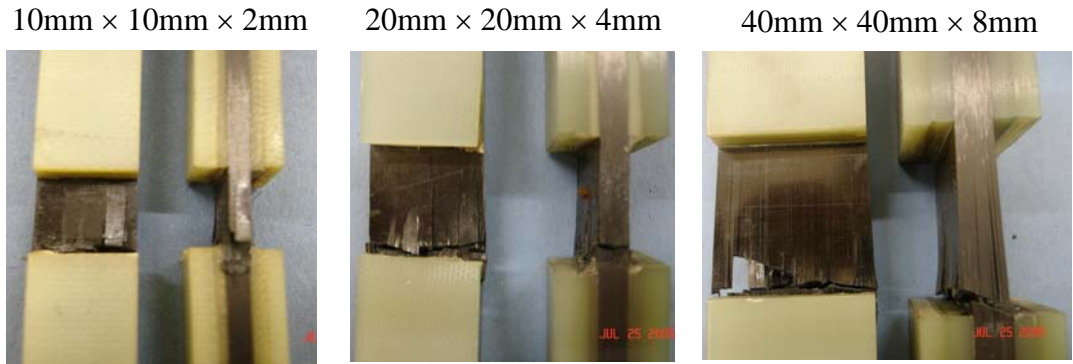


**Figure 7.** Typical overall failures of IM7/8552 unidirectional specimens. Front view and side view are shown for different thickness.

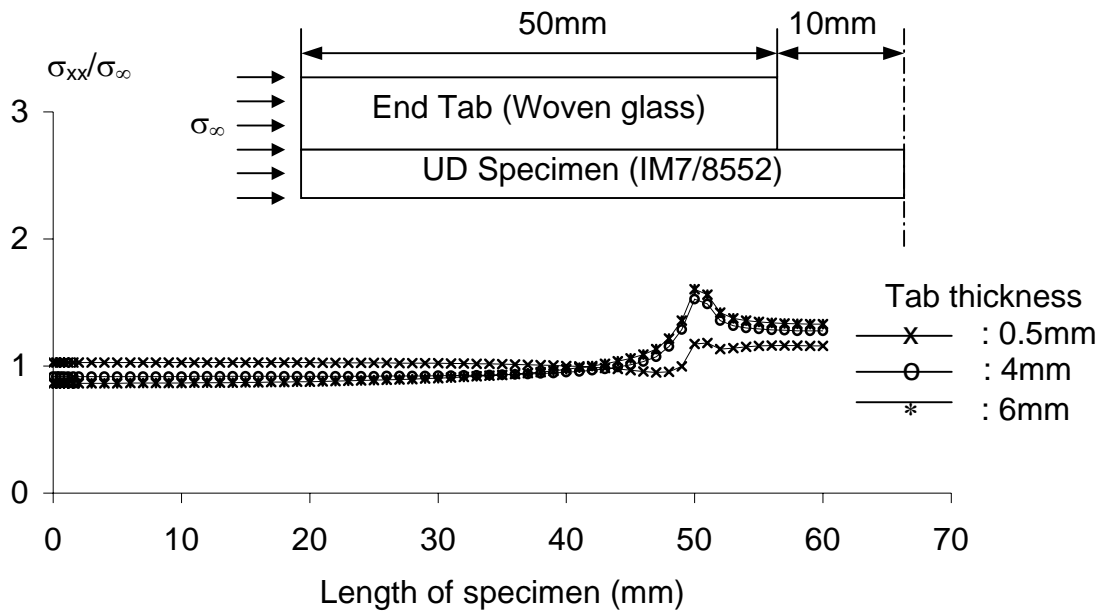
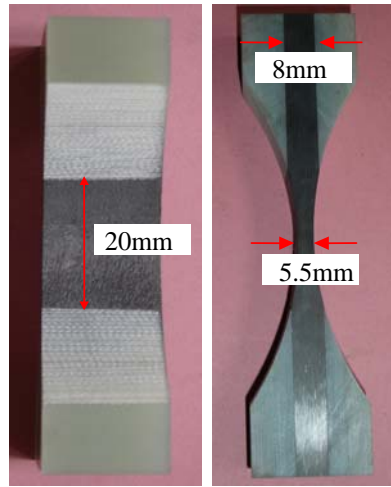


**Figure 8.** Stress distribution along the length of the specimen (IM7/8552 system). A high SCF develops at the gauge section-tab interface, especially for the 4mm and 6mm thick end tab.

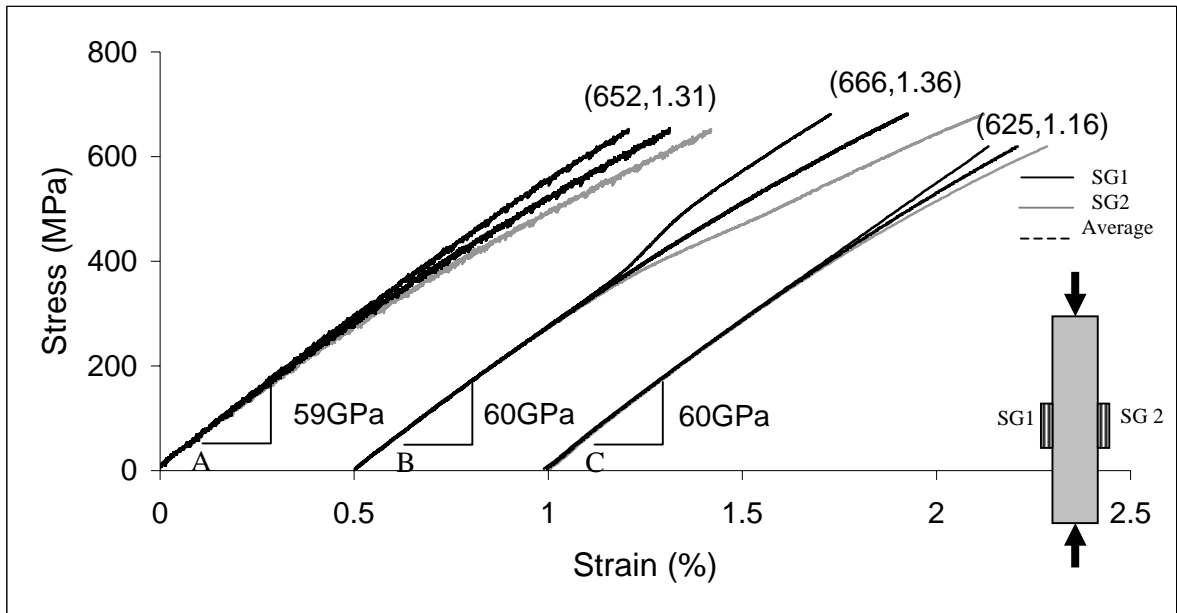


(a) Specimen dimensions

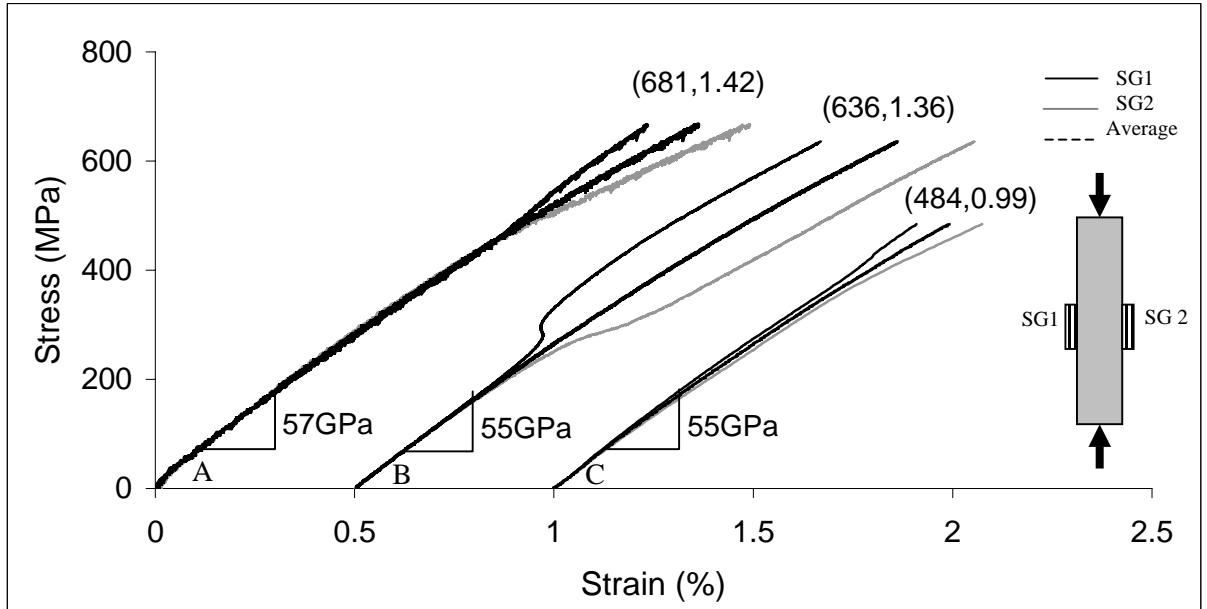


(b) Overall failure mode

**Figure 9.** a) Geometry and dimensions of the IM7/8552 waisted specimen and b) overall failure mode illustrating fracture within the gauge length due to fibre breakage and splitting.

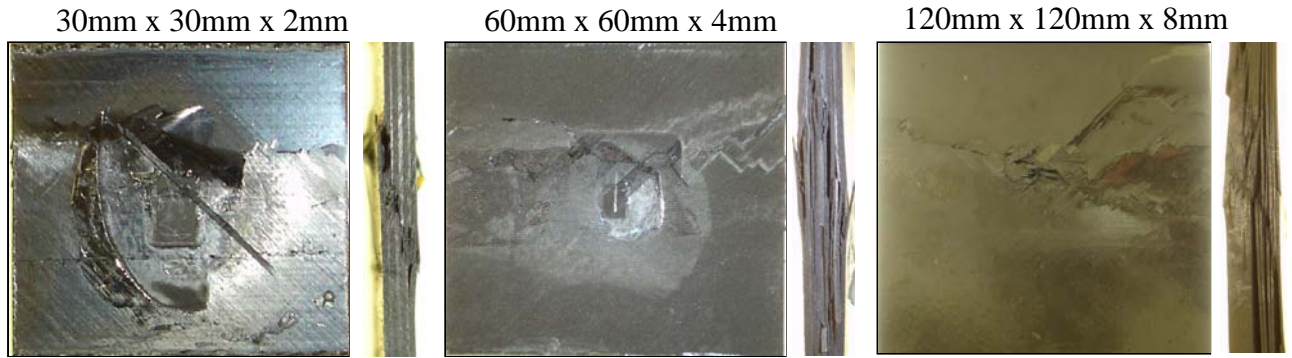


(a) Sublaminate-level scaled IM7/8522 ( $[45/90/-45/0]_{ns}$ ) laminate.



(b) Ply-level scaled IM7/8552 ( $[45_n/90_n/-45_n/0_n]_s$ ) laminate.

**Figure 10.** Stress-strain curves of the multidirectional IM7/8552 laminates (A= 2mm, B= 4mm and C= 8mm thick specimen)



(a) Sublaminate-level scaled IM7/8552  $[45/90/-45/0]_{ns}$  specimens



(b) Ply-level scaled IM7/8552  $[45_n/90_n/-45_n/0_n]_s$  specimens

**Figure 11.** Overall failure of multidirectional IM7/8552 specimens. Front view and side view are shown for different thicknesses (gauge length x width x thickness).

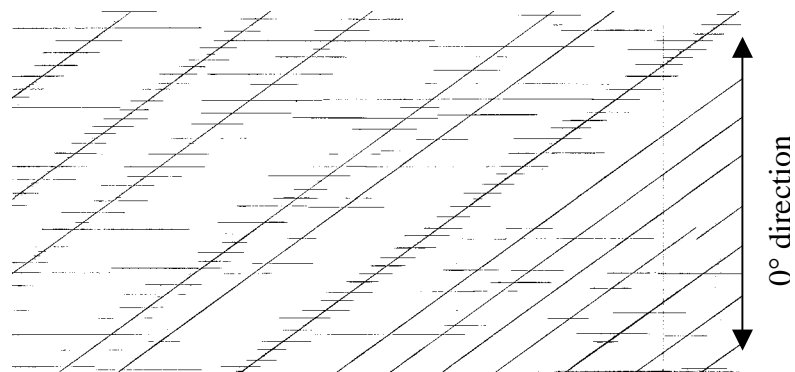


**Figure 12.** X-ray radiograph of an 8mm thick IM7/8552  $[45_8/90_8/-45_8/0_8]_s$  specimen before compression testing.

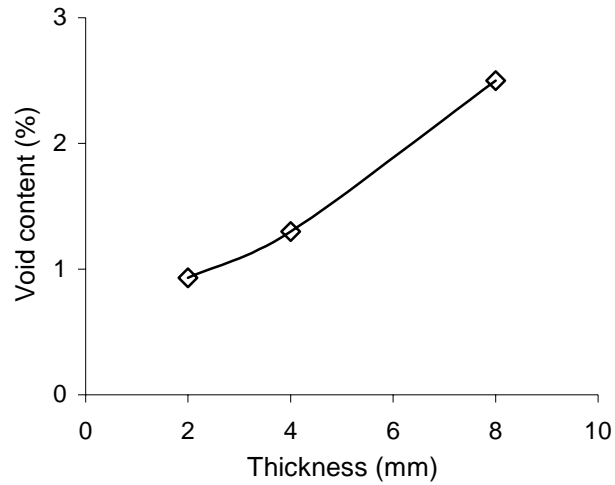


**Figure 13.** Void content versus specimen thickness (Carbon/epoxy unidirectional  $[0_4]_{ns}$  laminates)<sup>11</sup>.

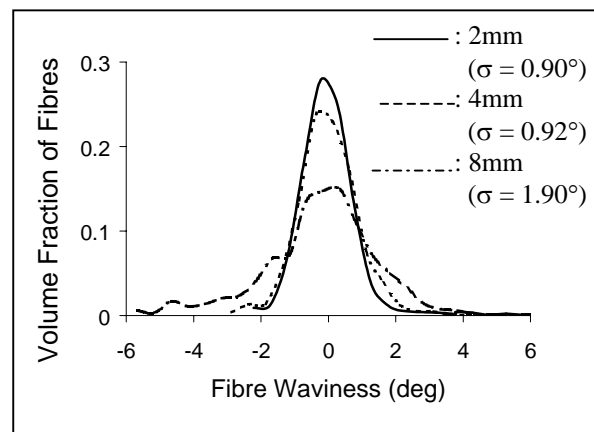


**Figure 14.** Fibre waviness distribution for 2mm, 4mm and 8mm thick carbon/epoxy  $[0_4]_{ns}$  unidirectional specimens<sup>11</sup>.

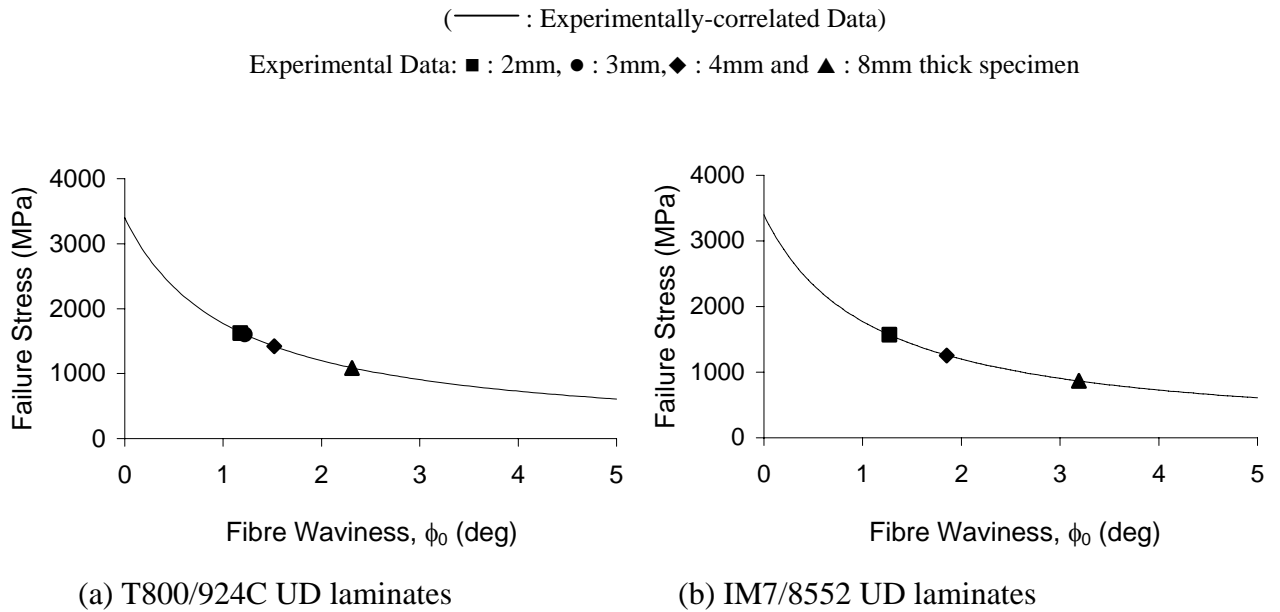


**Figure 15.** a) Variation of compressive strength with initial fibre waviness for a T800/924C unidirectional laminates and b) IM7/8552 unidirectional laminates.

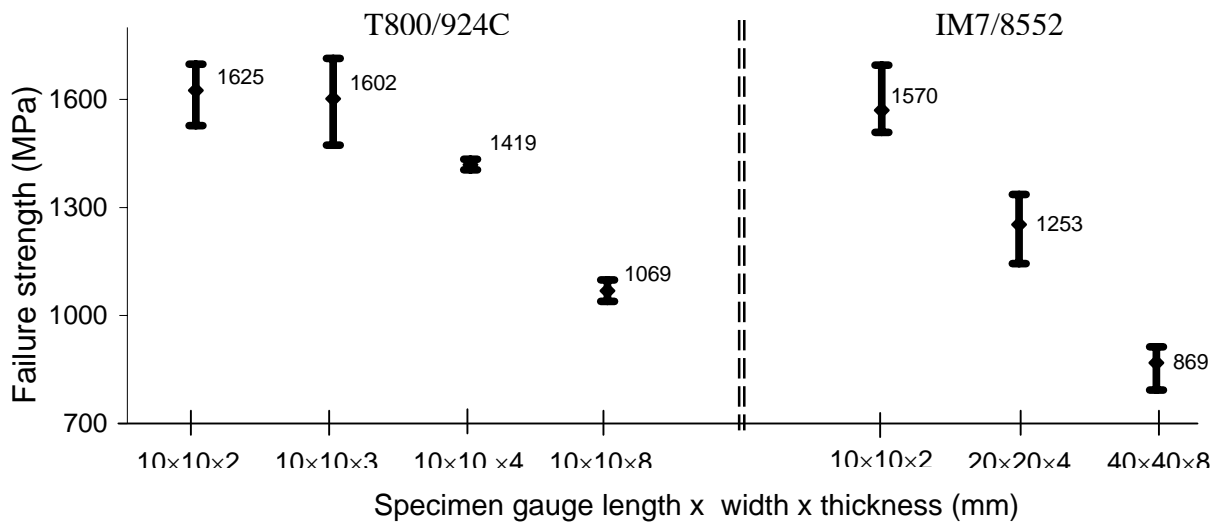


**Figure 16.** Comparison of average UD compressive strength as a function of specimen thickness (T800/924C)<sup>11</sup> and specimen volume (IM7/8552).

**Manuscript Ref: CSTE-D-06-00725**

Response to referee's comments:

We'd like to thank the reviewers for carefully considering our article, we found the comments/suggestions very useful and the manuscript has been amended accordingly.

Below is our response to reviewers' comments:

**Reviewer #1**

1. Standard FE analysis was performed using a commercially available package (ANSYS). Similar FE studies are reported in reference [21]. Additional information is given in the revised manuscript; see 1<sup>st</sup> paragraph of section 3 and section 4, page 18.
2. The validation or use of phenomenological rupture criteria is not the objective of the present work, however, the Budiansky fibre kinking analysis that identifies resin shear properties and fibre misalignment as critical parameters affecting failure strength are presented and discussed extensively in the manuscript.
3. All the corrections and improvements suggested have been implemented in the revised text.

**Reviewer #2**

1. In-plane and out-of-plane fibre microbuckling can occur in the testing of UD specimens. Text has been amended accordingly on page 11.
2. Even though the Weibull statistics could be used to explain the reduced strength in the UD specimens, the mode of failure is not a weakest link, but that affected by the stress concentration induced by the end tabs (see also [8, 21]). As explained in the discussion and concluding remarks sections these premature failures are not observed in the large sublaminar-level scaled multidirectional specimens where size effects are not observed.
3. The very short specimens, 10x10x2 mm, are those suggested by the ASTM standards and yes, end effects do exist and affect failure mode and strength. In the manuscript we emphasise the importance of careful specimen design and testing procedure. In the ICSTM test rig used in the present study the clamping blocks provide adequate lateral support and gripping, see section 2.3. A torque in the region of 10 Nm, as explained in the text, was applied. In the FE analysis an equivalent lateral pressure was applied to model the grips (clamping effect). Revised section 3 gives additional information on FE. See also section 4, page 18.
4. An anti-buckling device was used for the less stiff multidirectional specimens; text has been amended accordingly in paragraphs 2.2 and 2.3.
5. In the larger and thicker UD specimens the SCF influences the overall unidirectional behaviour by causing premature failures near the gripped region. Similar results and observations were reported in references [8, 21]. Such effects are not as severe in the multidirectional laminates (small or large size) where the off-axis surface plies do reduce the SCF and allow the 0-degree plies (the load carrying layers) to fail closer to their intrinsic strength, see sections 4 and 5.

6. Following the referee's comments additional clarifications have been inserted throughout the text. All identified typos have been corrected.